SNPO-C
FZR-351-1
15 DECEMBER 1967

NERVA IRRADIATION PROGRAM

GTR Test 21

Volume 1—Evaluation of a Polarographic Hydrogen-Gas Detector

Prepared for
Space Nuclear Propulsion Office
of the
National Aeronautics and Space Administration
Cleveland, Ohio 44135

Contract No. AF 29(601)-7077
Supplement 10

NUCLEAR AEROSPACE RESEARCH FACILITY

operated by

GENERAL DYNAMICS
Fort Worth Division

FZK-351-1
15 DECEMBER 1967

NUCLEAR AEROSPACE RESEARCH FACILITY

NERVA IRRADIATION PROGRAM

GTR Test 21

Volume 1—Evaluation of a Polarographic Hydrogen-Gas Detector

G. E. Irby
H. G. Carter
J. H. Lewis

Prepared for
Space Nuclear Propulsion Office
of the
National Aeronautics and Space Administration
Cleveland, Ohio 44135

Contract No. AF 29(601)-7077
Supplement 10

GENERAL DYNAMICS
Fort Worth Division

FOREWORD

The work described in this document was performed at the Nuclear Aerospace Research Facility (NARF) of the Fort Worth Division of General Dynamics for the Space Nuclear Propulsion Office, Cleveland, Ohio (SNPO-C) under Statement of Work No. 5 (Attachment I), Contract AF29(601)-7077, Supplemental Agreement No. 10.

The evaluation of the hydrogen-gas detector was performed as a part of GTR Test 21 which is the most recent of a series of tests being conducted on NERVA components and materials for SNPO-C. The other parts of GTR Test 21, which will be reported in separate volumes, are parahydrogen-orthohydrogen conversion, thermal conductivity and resistivity of materials, and materials structural properties.

Acknowledgment is given to Messers. Malbone Greene, Ray Wilson, and John Harmon of Beckman Instruments for their cooperation in explaining and demonstrating the theory, operation, and maintenance of the analyzer.

SUMMARY

A test has been conducted to evaluate the performance of a polarographic hydrogen-gas detector when subjected to various levels of reactor radiation. The detection system was designed and fabricated by Beckman Instruments, Inc. for the National Aeronautics and Space Administration.

One hydrogen sensor was irradiated with the Ground Test Reactor at several power levels from 4.4 kW to 4.4 MW (gamma dose rates of 2.3×10^6 to 2.3×10^9 ergs/g C-h). Cold nitrogen gas was used to cool the irradiated sensor. Sample gases containing 0.43, 1.08, or 2.47% hydrogen in air were supplied to the test sensor and a control sensor through a flow meter and gas distribution system. The response of the sensors (indicated percent hydrogen) and the response times were monitored as a function of reactor power level.

The principal effects observed with increasing exposure rate were: (1) a decrease in response, (2) an upscale zero shift, and (3) zero instability. The response had decreased by about 10% at an exposure rate of 2×10^8 ergs/g C-h, and at 2×10^9 ergs/g C-h the indicated hydrogen concentration with the 2.47-% sample gas was around 0.75%. A recovery of response occurred within minutes after cessation of the irradiation.

The total exposure to the sensor [2.43×10^9 ergs/g C and 2.61×10^{15} n/cm^2 (E>1.0 MeV)] was sufficient to cause the Delrin housing to embrittle and crack. The other organic materials appeared to be in relatively good condition, and ultimate failure of the sensor was due to loss of electrolyte via evaporation through the membrane. (Evaporation of the electrolyte is a characteristic of the sensor which limits its useful life.)

A theoretical analysis of the operating principle of the detector indicates that the observed results can be explained as being due to:

1. A radiation-induced steady-state increase in negative-ion concentration of the electrolyte resulting in a decrease in sensitivity.
2. A radiation-induced evolution of hydrogen gas in the electrolyte which produced the upscale zero shift.
3. Temperature fluctuations which affected the rate constant for radiation-induced ion production in the electrolyte with a resulting instability of response.

TABLE OF CONTENTS

TABLE OF CONTENTS (Cont'd)

LIST OF FIGURES

LIST OF TABLES

1. INTRODUCTION

The performance of a Beckman polarographic hydrogen-gas detector when exposed to a reactor radiation field has been evaluated. The test was performed at the Nuclear Aerospace Research Facility (NARF) on 8 September 1967 by irradiating a sensor with the Ground Test Reactor (GTR) at several power levels up to 4.35 MW. Gases with known percentages of hydrogen were used to determine the instrument performance as a function of reactor power level.

Beckman Instruments, Inc., designed and fabricated the detection system for the National Aeronautics and Space Administration under Contract NAS8-11940.

2. DESCRIPTION OF DETECTION SYSTEM

2.1 Sensor

A detailed description and discussion of the detection system is given in the Beckman final report (Ref. 1). Only a summary is given here. The sensor cell (Fig. 2.1) consists of an electrode cavity formed by an annular epoxy ring 2 in. in diameter by 0.7 in. thick. The cavity is capped on the aft end by a copper disc, and the forward end is closed by a gas-permeable membrane of 1-mil polystyrene film and a copper disc through which a hole is drilled to admit gas to the membrane. Three electrodes located in the cavity are immersed in an aqueous electrolyte of sulfuric acid and copper sulfate.

The anode is 0.040-in.-diam gold wire with a lightly platinized surface. The auxiliary and reference electrodes are circular loops of 0.040-in.-diam copper wire, 0.45 in. and 0.60 in. in diameter, respectively.

In the normal configuration, the sensor contains a heater for temperature control between -50°F and 86°F, and a thermistor for compensation at temperatures between 86°F and 120°F. The sensor used in this test did not have heaters since they were not to be subjected to low temperatures.

The entire sensor assembly is enclosed in a two-piece housing of Delrin. The rear cap covers the electrical terminals, and the forward cap is threaded and has a plastic plug which can

1. Screw
2. Washer
3. Detector, End, Rear
4. Leads, Wire
5. "O"-Ring
6. Screw, Packing
7. Spacer
8. "O"-Ring
9. Backing Plate
10. Body, Detector, Center
11. Electrode, Auxilliary
12. Electrode, Reference
13. Membrane, Polystyrene
14. "O"-Ring
15. Disc
16. Cap, Detector
17. Plug, Adjusting, Pressure
18. Screw
19. Screw, Flat Head
20. Membrane cover plate

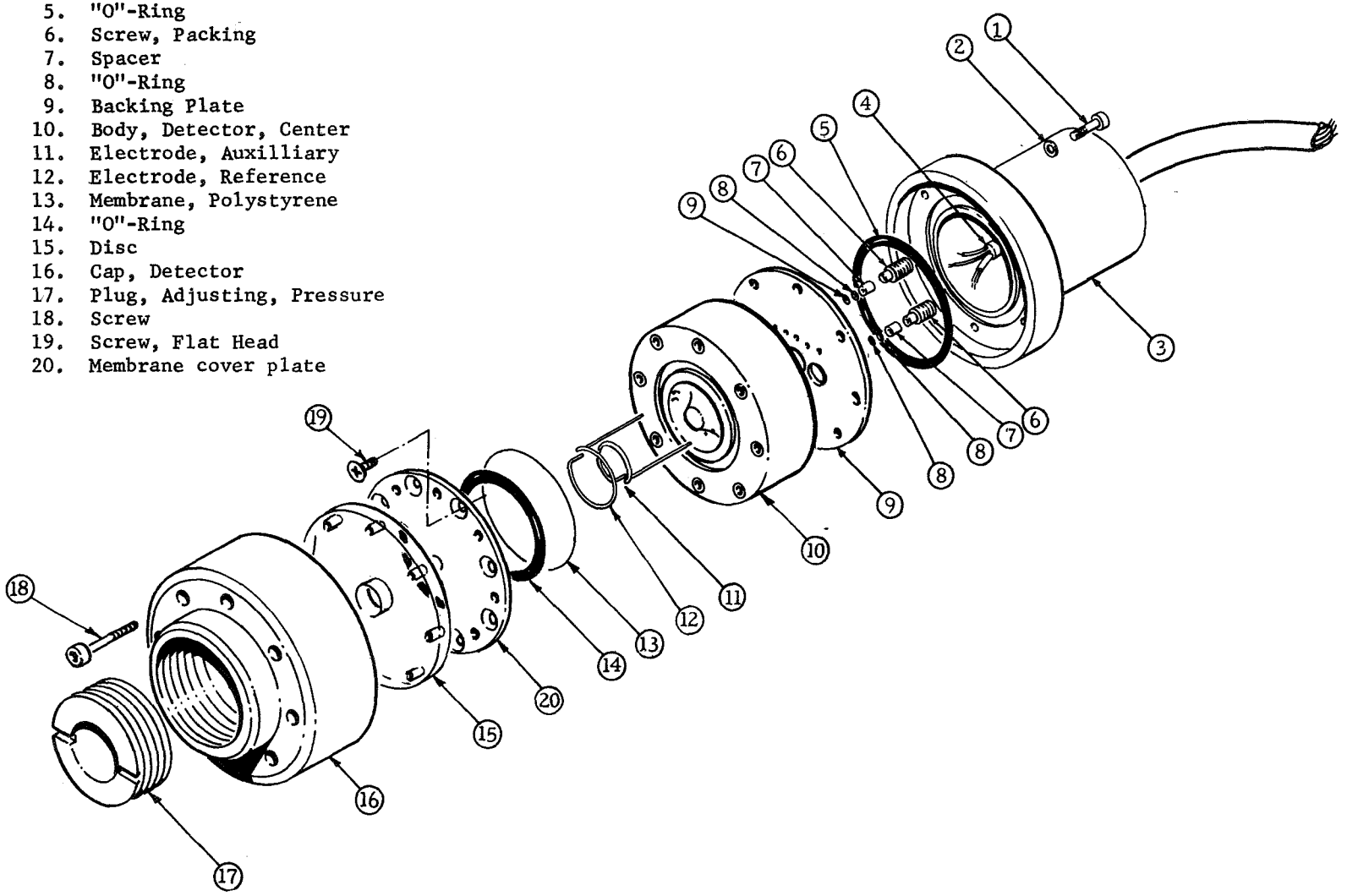

Figure 2-1 Exploded View of Polarographic Hydrogen Sensor (taken from Reference 1)

NA-2818

be adjusted to vary the thickness of electrolyte between the anode and membrane. The threaded plug presses against a Lucite disc covering the forward copper cover plate.

2.2 Principle of Operation

The following explanation of the operating principle is taken from Reference 1.

> The polarographic hydrogen detector is an electrochemical device that oxidizes hydrogen molecules to hydrogen ions at a catalytically active electrode surface and yields an electrical current that is proportional to the partial pressure of hydrogen gas in a sample gas mixture. The active electrode surface is exposed to the sample gas mixture by means of a semi-permeable membrane. The membrane also serves to contain the liquid electrolyte in the detector cartridge. Energy is supplied to the electrode system in order to maintain the rate of the reaction at a level that yields a linear calibration of detector output current with hydrogen concentration and the potentiostatic circuitry serves to control the sensor polarization voltage continuously at the experimentally determined optimal value. The rate of reaction established at the anode surface is of such a magnitude that it is always much greater than the rate at which hydrogen gas molecules diffuse through the semi-permeable membrane. Thus, the rate of response and sensitivity characteristics of the detector are completely established by the diffusion properties of hydrogen gas through the membrane and the geometry of the transducer and electrode system.

Hydrogen molecules which diffuse through the membrane are adsorbed on the anode and the electrochemical counterreaction occurs at the auxiliary electrode so that all current flowing is between these two electrodes through the electrolyte. This

current, which is proportional to the partial pressure of the hydrogen present, drives a meter which is calibrated in percent of lower explosive limit (LEL) of hydrogen in air. A change in barometric pressure in the vicinity of the sensor will be seen as an error in hydrogen concentration directly proportional to the barometric shift. Both channels tested had a sensitivity range of 0-100% LEL, or 0-4% hydrogen in air by volume.

The third electrode is for the purpose of maintaining a reference potential for the electrochemical cell. The anode is kept at 450 mV positive with respect to the reference electrode. In order to keep the anode constantly catalytically active, a 10-msec, 800-mV anodic pulse followed by a 20-msec, 200-mV cathodic pulse is applied to the anode once every 20 sec. During this pulsing, the meter circuit is clamped off to mask the transient.

2.3 Instrumentation

The instrumentation for each hydrogen sensor is contained in a module and consists of the following functional groupings:

a. The potentiostatic circuitry

b. Current amplification, memory, and temperature compensation circuitry

c. Biasing and reactivation pulsing circuitry

d. Power supplies and heater circuitry

e. Readout and alarm circuitry

The operation of these circuits is described in Reference 1. The controls of particular interest insofar as the results of this experiment are concerned are the potentiometers for current-amplifier gain and recorder zeroing.

3. EXPERIMENTAL PROCEDURES

3.1 Sensor Setup

3.1.1 Temperature Control

The upper temperature limit of the sensor is about 120°F and a desirable operating temperature is around 86°F. Since considerable nuclear heating was expected during the irradiation, the sensor was enclosed in a cylindrical copper shroud closed on the ends with two fins approximately 6 in. in diameter. The annular fins were made to slip over the front and rear caps of the sensor. They were attached to the internal copper plates by means of the cell assembly screws; a heat conduction path was thus provided, via the screws, from the copper plates to the fins.

Coolant gas to the shroud was supplied from the gas phase of a liquid-nitrogen storage tank through an insulated line. A proportional cryogenic valve operated manually from a Bristol controller regulated the quantity of coolant gas.

Temperatures were measured at three locations. One copper-constantan thermocouple was placed inside the shroud to monitor gas temperature, and one was placed in contact with the Delrin housing behind the electrolyte chamber. The third thermocouple, which was used as the temperature-control point, was placed against the front copper plate through a small hole drilled in the

front Lucite disc. The thermocouple was then potted into the hole to hold it in position against the copper plate for good thermal contact.

3.1.2 Irradiation Configuration

The sensor was mounted in a framework to position it at the west face of the Ground Test Reactor (GTR) on the core centerline. The sensor was positioned with the axis pointing toward the reactor with the electrolytic cavity approximately 6 in. from the wall of the reactor closet. The line supplying the test gas was arranged so as to exhaust the gas directly into the opening of the sensor.

3.1.3 Control Configuration

A second sensor was set up on the north ramp outside the reactor shield. The control-sensor setup differed from the test-sensor setup only in that no cooling was provided. This sensor was at ambient-air temperature ($\sim 80^{\circ}F$). Test gas was provided by the same system.

3.2 Test-Gas System

The system for metering the test gas to the sensors is shown in Figure 3.1. Bottled gas with certified analysis of 0.43, 1.08, or 2.47% hydrogen by volume in air was supplied through a regulator and flow meter (Brooks Rotameter, Size R-2-15C) to either sensor by the appropriate setting of valves.

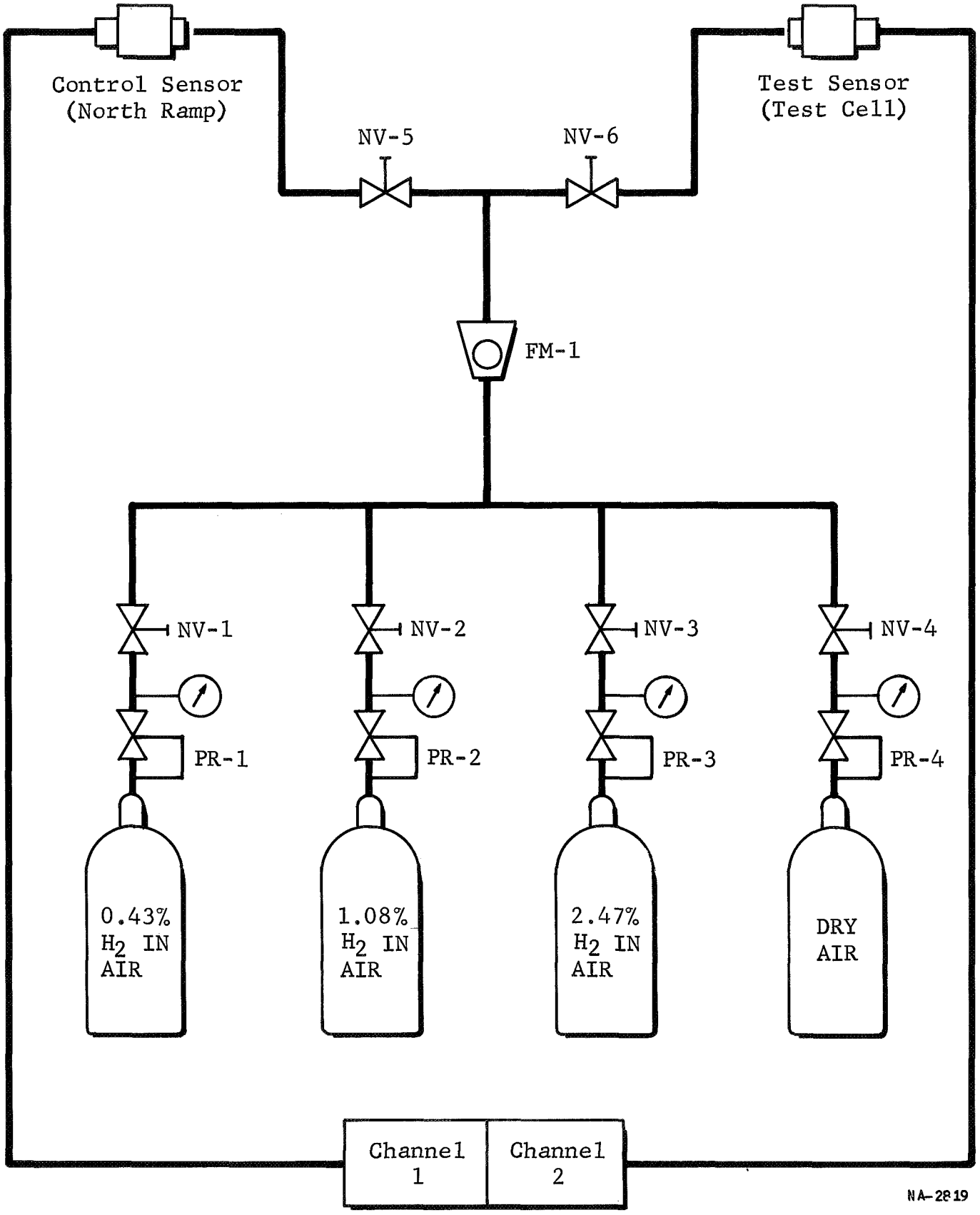

Figure 3-1 Schematic of Gas Metering System

The flow meter and valves were panel mounted in the test console with the gas bottles located nearby.

3.3 Test Procedure

With the analyzer system checked out and operating properly, the test sensor was moved into position adjacent to the reactor. Both channels were then calibrated by flowing 0.26 ft^3/min of test gas containing 2.47% hydrogen to the sensor and adjusting the gain of the amplifiers so as to have a meter reading of 2.50%. The gases with 1.08 and 0.43% hydrogen were then supplied to the sensors, in turn, and the meter readings recorded. Several data cycles were taken prior to the irradiation in order to check reproducibility.

The reactor was then operated at the power levels given in Table 3.1. The time at each power level and the megawatt minutes accumulated are also given.

At each power level, the coolant gas was regulated so as to maintain a temperature of about 75°F at the copper plate over the front of the electrolyte chamber; the actual temperatures obtained during various data cycles ranged from 64° to 80°F.

Following the 4.35-MW irradiation, the reactor was retracted from the closet to reduce the radiation level at the sensor to a low value and data cycles were run for 40 min. The reactor was then moved back into the irradiation position and

Table 3-1

GAMMA AND NEUTRON EXPOSURE[a]

Time Interval (CDT)	Power Level (MW)	Integrated Power (MW min)	Gamma Dose (erg/g C)	Neutron Fluence E>1.0 MeV (n/cm^2)
1903-1916	0.0044	0.057	4.9×10^5	5.3×10^{11}
1916-1927	0.013	0.20	1.73×10^6	1.87×10^{12}
1927-1950	0.044	1.21	1.05×10^7	1.13×10^{13}
1950-2007	0.44	8.69	7.53	8.11
2007-2028	0.87	27.0	2.34×10^8	2.52×10^{14}
2028-2046	1.76	58.6	5.08	5.47
2046-2102	2.64	100.9	8.75	9.41
2102-2113	3.50	139.4	1.21×10^9	1.30×10^{15}
2113-2129	4.40	209.8	1.82	1.96
2129-2210	0.0	209.8	1.82	1.96
2210-2220	0.44	214.2	1.86	2.00
2220-2226	0.87	219.4	1.90	2.05
2226-2233	1.74	231.6	2.01	2.16
2233-2244	4.35	280.0	2.43	2.61

[a] Estimated from GTR mapping data.

several more data cycles were obtained at power levels of 0.44, 0.87, 1.74 and 4.35 MW.

Several data cycles were taken immediately after completion of the irradiation, and the system was then checked for several more days. Some additional data were also obtained in the form of meter reading vs temperature of the sensor and meter reading vs zero-potentiometer setting.

3.4 Data Acquisition

The parameters monitored during the test were:

1. Temperatures of the copper plate, cooling gas, and exterior wall temperature of the test sensor, and wall temperature of the control sensor
2. Zero drift of the entire measuring system
3. Zero drift of the electronics only
4. Reference potential being applied to the sensor
5. Polarization pulses being applied to the sensor
6. Response at each of the three test-gas concentrations
7. Response time (time to reach 90% of maximum reading) at the 2.47% hydrogen concentration

The reference potential was measured with an NLS Model M24 digital voltmeter. The waveform of the polarization pulse was recorded on a Tektronix Model 564 storage oscilloscope and photographed periodically. Zero drift of the electronics was checked occasionally by use of the "Calibrate" position of the

function switch which substitutes an internal dummy for the sensor. The response time was measured with a stop watch. The system was purged and the 2.47% hydrogen turned on; the stop watch was started at the moment the meter began deflecting and was stopped when the preselected value was reached. With increasing reactor power levels, the zero began drifting uprange. It was decided that the best way to handle this problem was to leave the gain adjustment at the initial setting and rezero the meter prior to each data cycle. The calibrated potentiometer knobs made it possible to log these adjustments and later account for their effect on the data.

A typical data cycle consisted of the following steps:

a. Record temperatures

b. Purge with dry air

c. Measure and record the reference potential

d. Adjust the zero of the LEL meter and record the potentiometer setting

e. Check the calibration reading and record the potentiometer setting

f. Flow 0.43%-hydrogen gas at a rate of 0.26 ft^3/min and record the LEL reading after approximately 30 sec

g. Repeat Step f with 1.08% hydrogen gas

h. Repeat Step f with 2.47% hydrogen gas

i. Purge with dry air

j. Flow 2.47%-hydrogen gas at a rate of 0.26 ft^3/min and measure and record the response time; record the LEL reading after approximately 30 sec

k. Photograph (occasionally) the wave form of the polarization pulse

4. RESULTS AND DISCUSSION

4.1 Results

Of the seven monitored parameters, the reference potential, the polarization pulse, and the zero drift of the electronics were quite stable. The reference potential remained at 450 $\pm$ 2 mV throughout the course of the test, and the pulse waveform was also unchanged as shown by a comparison of the photographs. The behaviors of the remaining four parameters - sensitivity, zero drift of the system, response time, and temperatures - are presented and discussed in this section.

The response data for the test sensor are given in Table 4-1 and are plotted in Figure 4-1 as a function of the gamma dose rate. The temperature measured at the front copper plate of the sensor is also given in Table 4-1, as is the setting of the zeroing potentiometer prior to each data cycle. While the temperature sensitivity of the detector is pronounced (Fig. 4-2), the data have not been corrected for temperature variations. Temperature effects are discussed in Section 5.

Figure 4-3 shows the meter readings as a function of the zeroing-potentiometer setting. Figure 4-4 shows the unadjusted zero reading (without test gas) as a function of gamma dose rate; the slope of the "zero position" curve of Figure 4-3 was used to compute the meter reading from the zero-potentiometer settings

Table 4-1

DATA FOR TEST SENSOR

Date/ Time	Power Level (MW)	Zero-Pot. Setting	Response			Temperature of Cu Plate (°F)
			0.43% H	1.08% H	2.47% H	
9-8-67						
1655	0	4.95	0.34	0.98	2.48	64
1703	0	4.97	0.37	1.02	2.52	64
1725	0	4.97	0.32	0.95	2.40	60
1830	0	4.98	0.32	1.0	2.50	68
1836	0	4.98	0.31	0.98	2.42	
1904	0.0044	4.99	0.35	1.0	2.51	62
1908	0.0044	4.99	0.31	0.98	2.45	68
1918	0.013	4.98	0.31	0.94	2.40	64
1922	0.013	4.98	0.31	0.93	2.45	64
1935	0.044	4.98	0.30	0.89	2.25	58
1940	0.044	4.98	0.33	0.98	2.40	64
1944	0.044	4.98	0.30	0.98	2.40	64
1951	0.44	4.92	0.32	0.95	2.33	70
1955	0.44	4.92	0.30	0.88	2.22	69
2000	0.44	4.92	0.30	0.90	2.20	70
2009	0.87	4.87	0.30	0.80	2.0	67
2015	0.87	4.84	0.23	0.70	1.77	65
2019	0.87	4.87	0.20	0.62	1.65	64
2030	1.76	4.69	0.30	0.83	1.90	69
2041	1.76	4.76	0.15	0.53	1.51	66

Table 4-1 (Cont'd)

Date/ Time	Power Level (MW)	Zero-Pot. Setting	Response			Temperature of Cu Plate (°F)
			0.43% H	1.08% H	2.47% H	
2050	2.64	4.61	*	0.35	0.90	80
2057	2.64	4.70		0.38	0.98	68
2104	3.50	4.63		0.33	0.90	70
2108	3.50	4.63		0.28	0.78	73
2115	4.40	4.63		0.05	0.20	66
2118	4.40	4.65		0.10	0.42	66
2123	4.40	4.48		0.30	0.70	83
2125	4.40	4.48		0.20	0.50	80
2128	5.00				0.50	70
2145	0	4.70		0.60	1.50	63
2155	0	4.70		0.65	1.65	68
2202	0	4.68		0.62	1.55	70
2215	0.44	4.52		0.50	1.30	76
2221	0.87	4.52		0.48	1.22	74
2226	1.74	4.42		0.50	1.28	74
2229	1.74	4.42		0.43	1.20	74
2234	4.35	3.93		0.33	0.89	86
2237	4.35	3.88		1.8	1.90	90
2241	4.35	4.18				90
2250	0	4.83		0.92	2.50	87
2252	0	4.83		0.95	2.50	84
2258	0	4.83		0.92	2.40	82
9-9-67						
1138	0	4.95		0.75	2.10	76

Table 4-1 (Cont'd)

Date/ Time	Power Level (MW)	Zero Pot. Setting	Response			Temperature of Cu Plate (°F)
			0.43% H	1.08% H	2.47% H	
1147	0	4.95	*	0.83	2.15	76
1208					2.28	
9-11-67						
2207	0	4.96		0.65	1.89	76
9-12-67						
2110	0	4.96		0.50	1.7	72

* Discontinued because of limited quantity of gas.

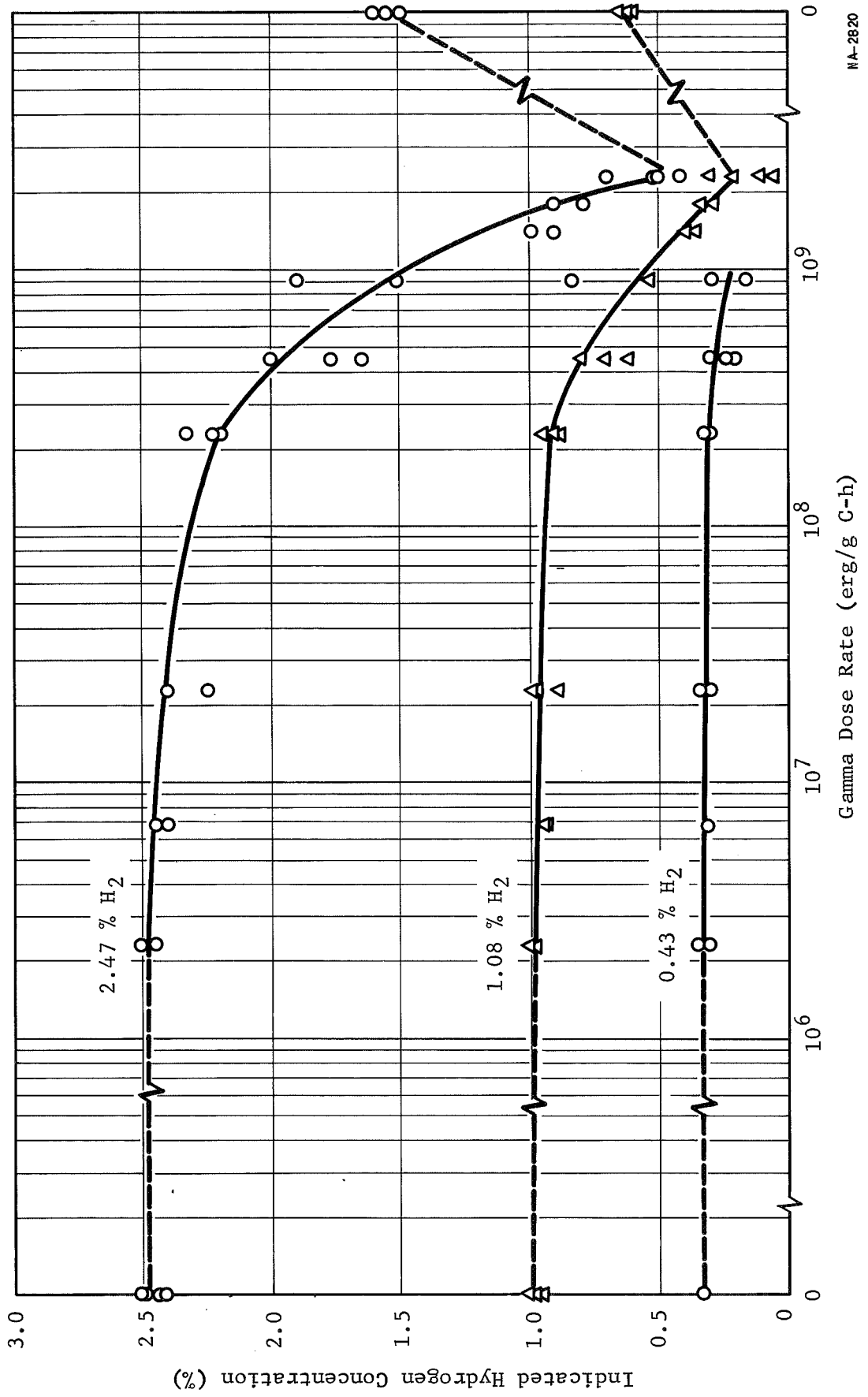

Figure 4-1 Response of the Hydrogen Sensor as a Function of Gamma Dose Rate

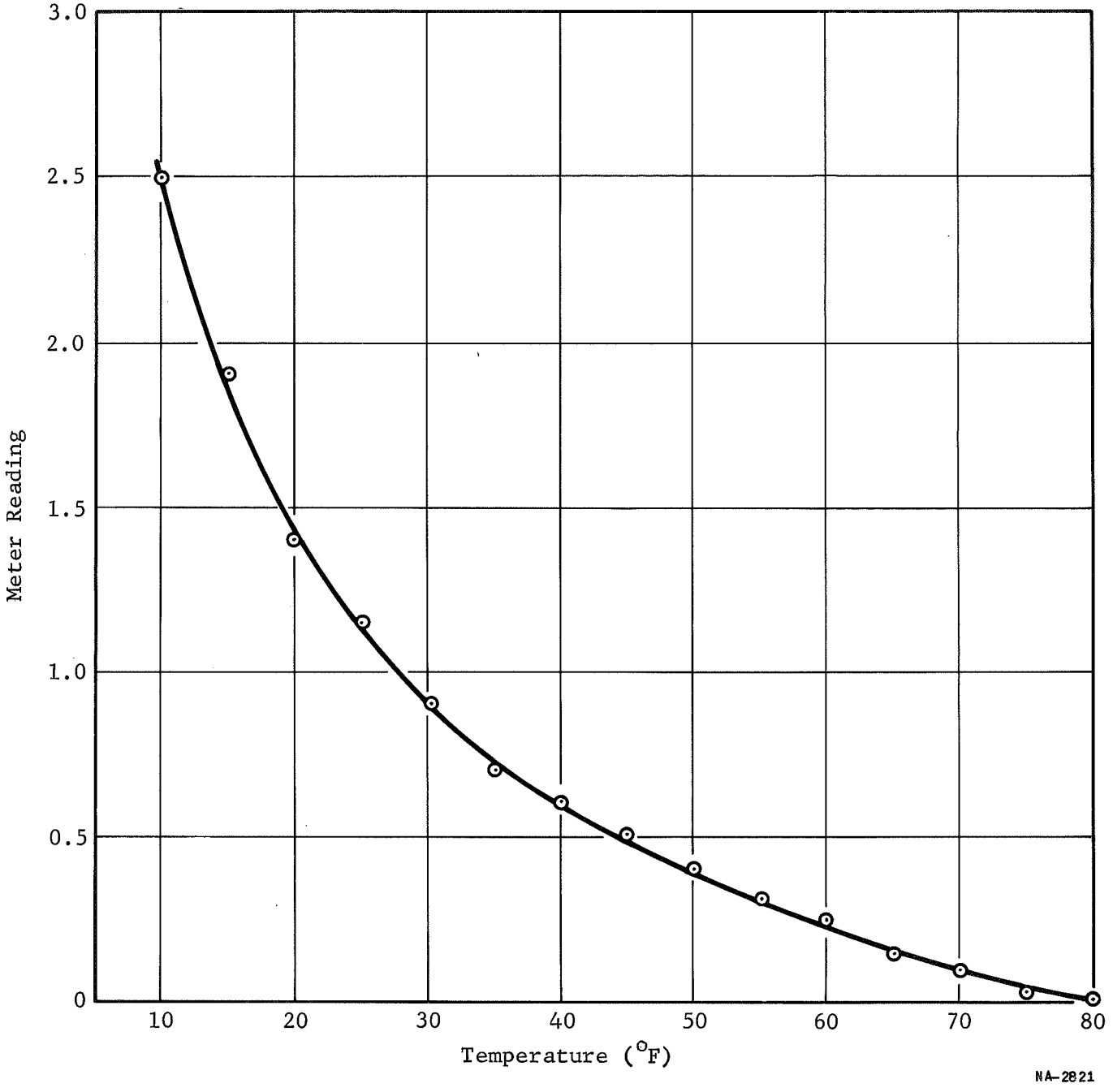

Figure 4-2 Temperature Response of Hydrogen Sensor

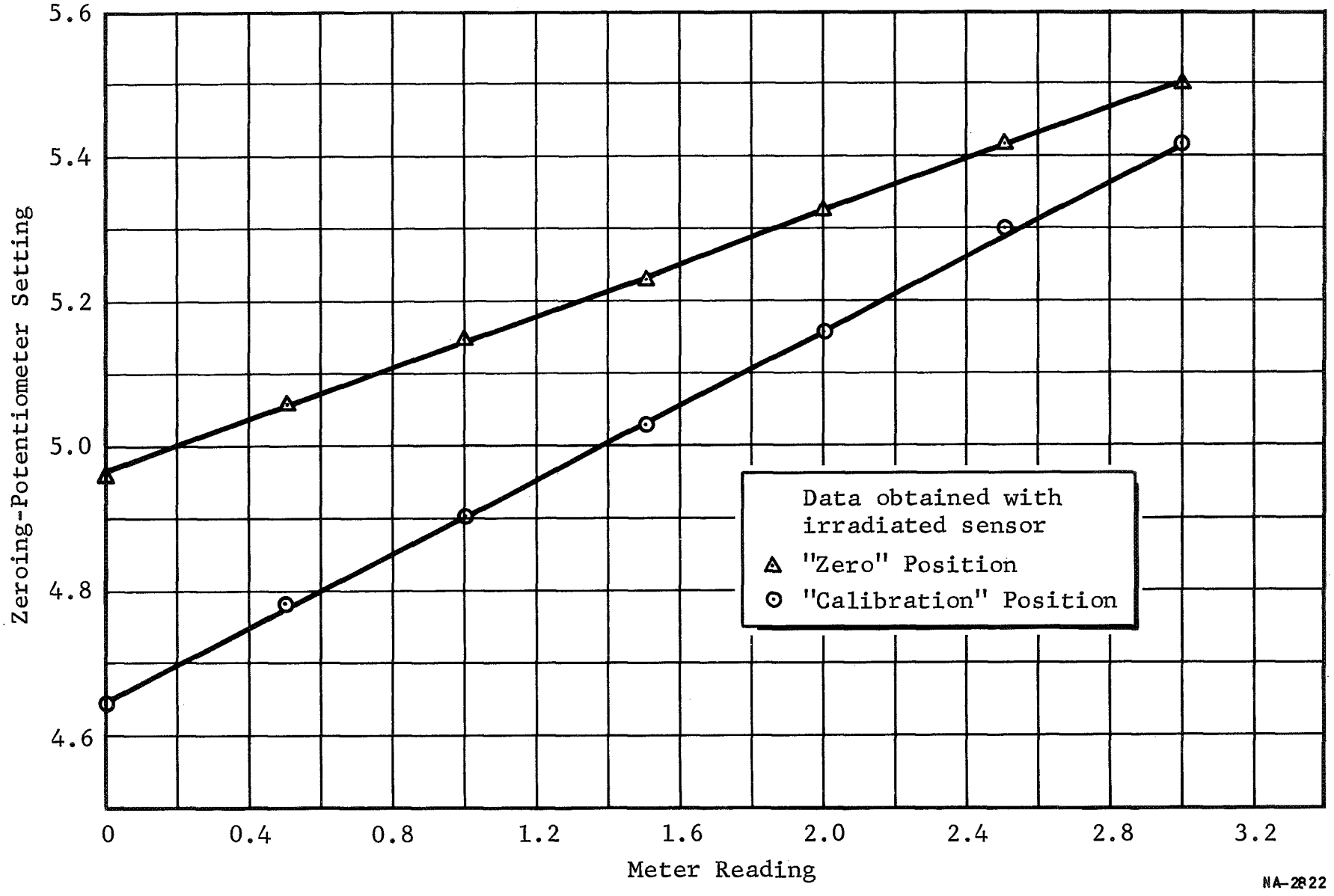

Figure 4-3 Meter Reading as a Function of the Zeroing-Potentiometer Setting

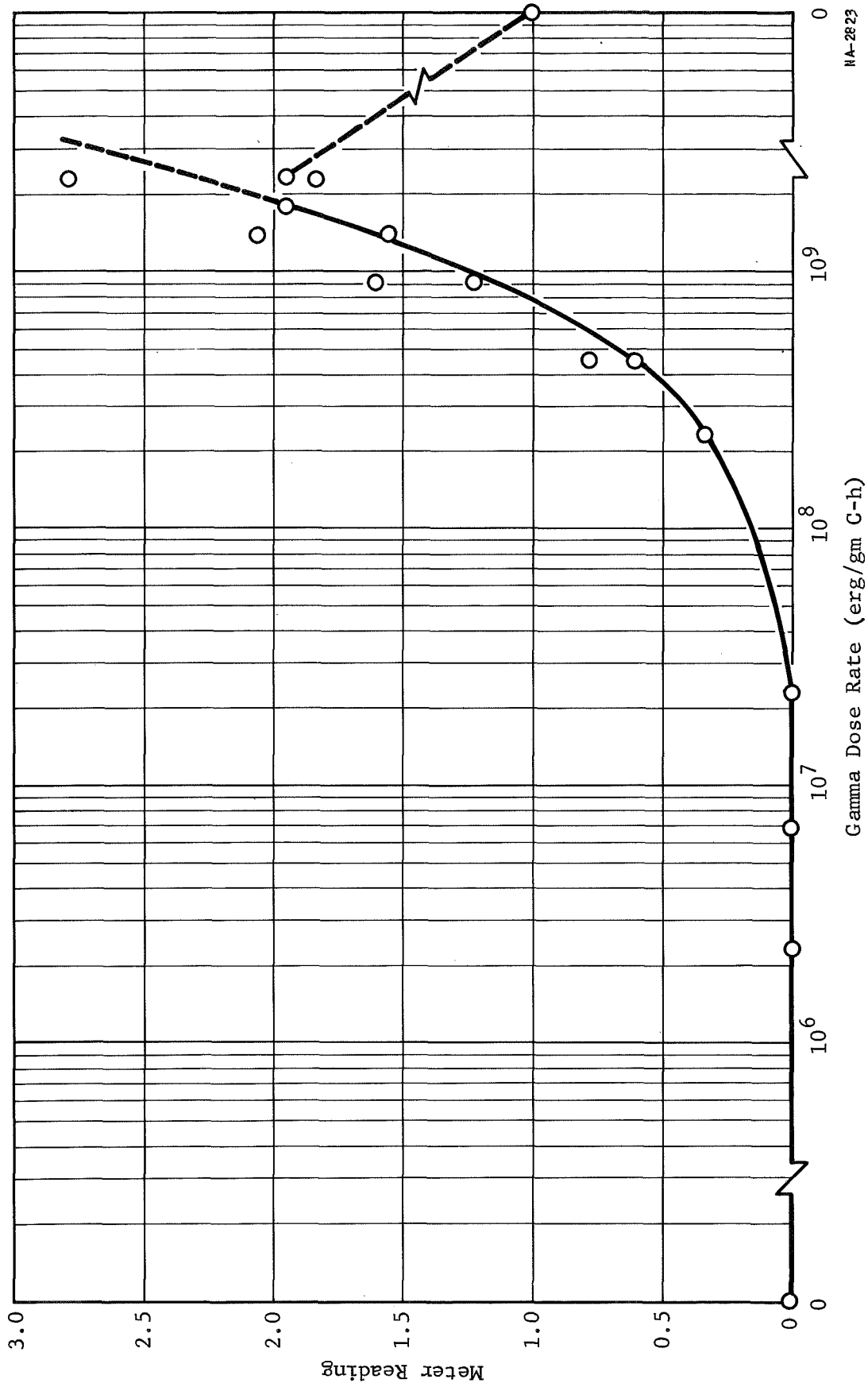

Figure 4-4 Meter Reading in the Absence of Sample Gas as a Function of Gamma Dose Rate

given in Table 4-1. The data in Figures 4-2 and 4-3 were obtained with the test sensor after completion of the irradiation. Also, in obtaining the data of Figure 4-2, the sensor was cooled slowly with no attempt being made to allow temperature equilibrium to be established throughout the sensor; the reason for this was to more or less simulate the conditions prevailing during the irradiation test in which power levels, and consequently temperatures, were changed every 10-15 min.

Table 4-2 gives the response time at each reactor power level through 0.44 MW. The response of the instrument is exponential, and the time constant is arbitrarily taken as the time to reach 90% of the final value, or 90% of 2.50 in this case. However, because the sensitivity decreased with power level, a point was soon reached at which the final reading did not reach 90% of 2.50. At that time, the time constant was taken as the time to reach 90% of the final reading, no matter what it was. With this definition, the time constant was found to remain in the 4- to 10-sec range. The time constant measured by means of a stop watch depended quite critically on the meter zero; if the zero happened to drift down while the measurement was being made, the time constant was lengthened appreciably. A more accurate procedure would probably have been to record the sensor output on a strip-chart recorder.

Table 4-2

RESPONSE TIME OF TEST SENSOR

Time	Power Level (MW)	Response Time* (sec)	Response with 2.47% H_2
1650	0	2.6	
1655	0	3.2	2.42
1703	0	2.8	2.51
1725	0	2.8	-
1830	0	3.3	2.48
1904	0.0044	3.5	2.49
1908	0.0044	3.8	2.45
1918	0.013	6.5	2.38
1922	0.013	8.0	2.35
1935	0.044	9.2	2.33
1940	0.044	6.5	2.40
1944	0.044	6.0	2.40
1951	0.44	11.6	2.30
1955	0.44	19.0	2.26
2000	0.44	28	-

* Time to reach 90% of 2.50.

Table 4-3 contains the sensitivity data for the control channel. This instrument had an appreciable and erratic zero drift even in the absence of radiation; the time constant remained relatively constant, however, ranging from 2.5 to 3.8 sec.

It should be noted that although the sensor is temperature compensated above about 86°F by use of a thermistor, there is no direct information as to the actual temperature of the electrolyte or the thermistor. Since the reactor power was changed every 15 to 20 min, it is quite likely that the temperature measured at the front copper plate was not the same as at other points in the sensor. This would have resulted in a tracking error between the thermistor and the thermocouple on the copper plate. Had sufficient time been allowed for thermal equilibrium to be reached, Figure 4-2 would probably have been much flatter. For this reason, no temperature correction has been applied to the data.

4.2 Discussion of Results

The main effects observed during and after the test were:

a. A decrease in response (or indicated hydrogen concentration) with increasing exposure rate

b. An increase in upscale zero drift with increasing exposure rate

c. An increasing instability of the zero with increasing exposure rate

Table 4-3

DATA FOR CONTROL SENSOR

Date/ Time	Zero-Pot. Setting	Sensitivity			Temperature (°F)
		0.43%H	1.08%H	2.47%H	
9-8-67					
1534	5.05	0.35	1.1	2.50	81
1600	5.07	0.42	1.15	2.70	81
1608	5.05	0.40	1.08	2.60	81
1615	5.06	0.30	0.90	2.40	81
1840	5.09	0.33	0.99	2.49	80
1847	5.09	0.32	0.98	2.50	80
1912	5.09	0.33	1.0	2.50	80
1925	5.06	0.29	0.90	2.37	80
2140	5.15		0.90	2.30	76
2145	5.20	0.30	0.93	2.40	76
9-9-67					
1118	5.0	0.37	1.0	2.50	81
1129	5.0		1.04	2.60	81
9-11-67					
2155	4.95		0.70	2.11	76
9-12-67					
1900	4.95		0.65	2.00	87

d. A fairly rapid recovery of performance following cessation of irradiation

e. A rather severe degradation of the Delrin housing

f. A large gas bubble in the electrolyte

As seen from Figure 4-1, the sensitivity had decreased about 10% at an exposure rate of 2×10^8 erg/g C-h, and the response is, approximately at least, an exponentially decreasing function of gamma dose rate (see Sec. 5). (It should be noted, however, that the same result would be obtained by plotting response vs neutron flux. It has been estimated that the energy deposition rate from neutrons is 25% of that for gamma rays in the electrolytic solution.)

The upscale drift of the meter reading (with no hydrogen gas) above a dose rate of about 10^8 erg/g C responded rapidly to changes in power level. The higher the power level, the more unstable the zero reading was, and it was virtually impossible to complete a data cycle without the zero drifting up or down by an indicated 0.1 to 0.2%. This drift accounts for much of the scatter in the data points.

In addition to outgassing hydrogen when irradiated, the plastic materials used in the construction of the sensor are subject to physical degradation at relatively low exposure levels.

Although the Delrin housing was embrittled and badly cracked (Figs. 4-5 and 4-6), the other organics appeared to be in satisfactory condition.

Upon disassembling the sensor, it was found that a large gas bubble had formed in the electrolyte. There is no way of knowing when the bubble formed, but since the electrolyte can evaporate through the membrane, it is probable that most of the loss of electrolyte occurred during the several days that elapsed between the irradiation and inspection of the sensor. Both of the sensors had been freshly charged with electrolyte two days prior to the irradiation. The sensors have a mean life of about 10 to 14 days due to evaporation of the electrolyte which occurrs in the absence of irradiation, although the evaporation rate is probably increased by irradiation.

A check of the condition of the electrolyte can be made by measuring its ac impedance. Both sensors had an impedance of 30 kΩ when freshly charged. At the start of the test 50 h later, the test and control sensors had impedances of 43 and 50 kΩ, respectively. At the conclusion of the irradiation, the impedance of the test sensor was 20 kΩ and that of the control sensor was 80 kΩ. After 70 h, impedances were 62 and 81 kΩ, and at 190 h they were greater than 1 MΩ and 95 kΩ for the test and control sensors, respectively.

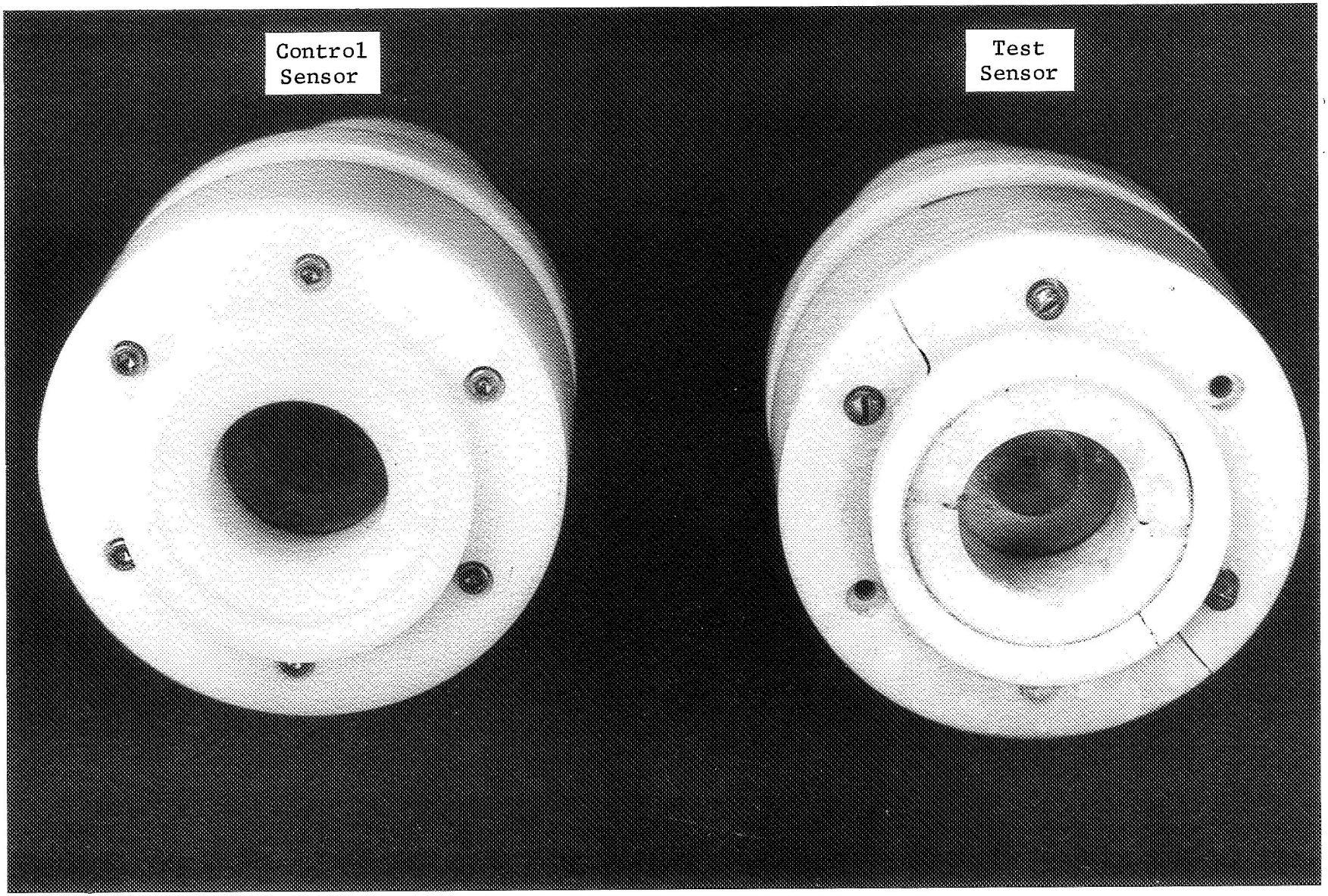

Figure 4-5 Front View of Control and Test Sensors

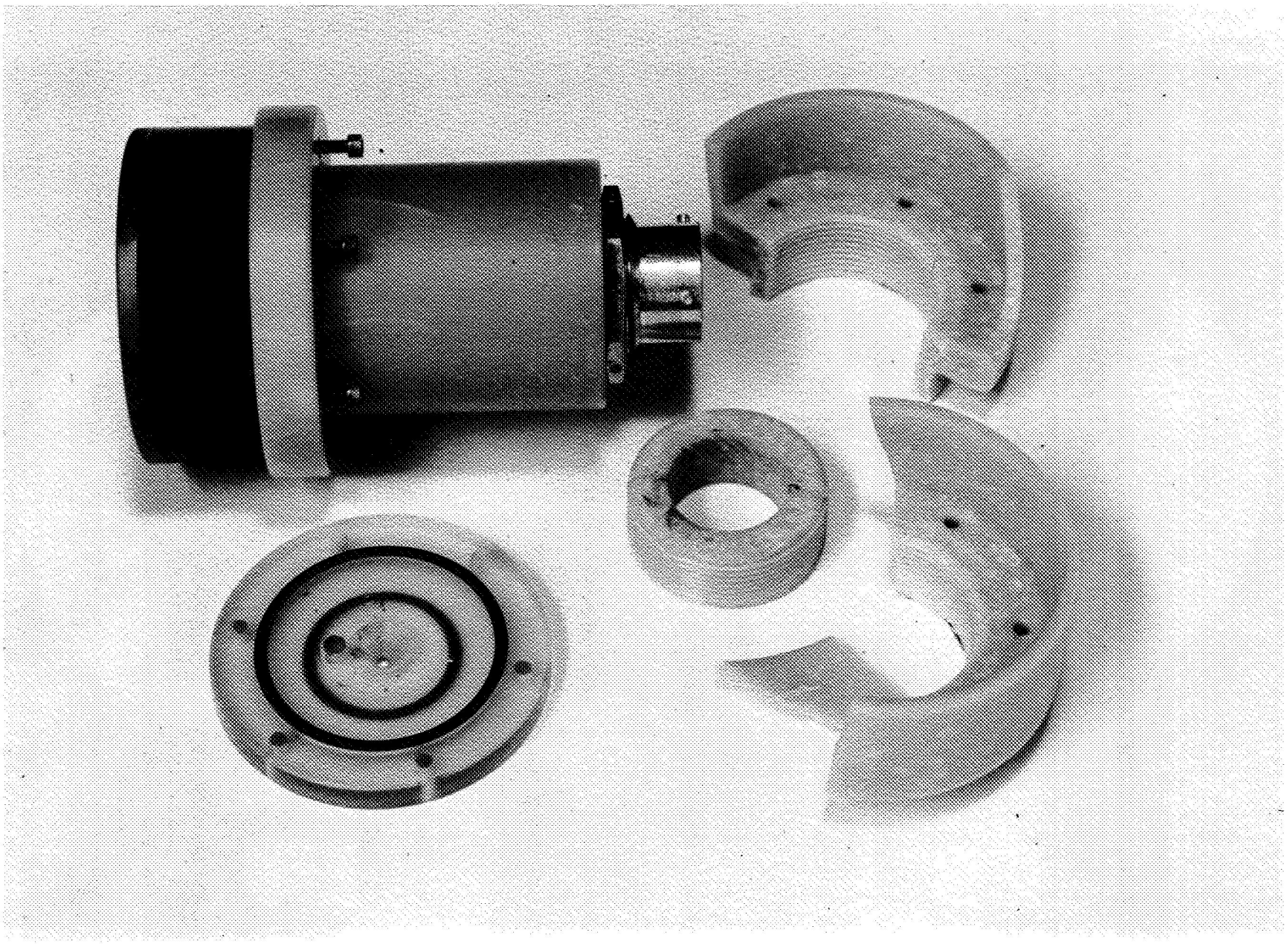

NA-2825

Figure 4-6 Test Sensor Showing Fractured Housing

5. ANALYSIS OF RESULTS

5.1 Analytical Approach

In the following discussion, an explanation is offered for the main effects listed in Section 4.2. In spite of the considerable scattering of data at the higher dose-rate levels, it is felt that the magnitudes of effects (a) and (b), as a function of dose rate, are explained quantitatively by the analysis given in Section 5.2. A non-quantitative and therefore tentative explanation of effects (c) and (d) is given in Section 5.3. Section 5.4 offers a few suggestions which might conceivably be implemented in the operation of the Beckman analyzer to make it more suitable for use in radiation fields of dose rate higher than 2×10^7 erg/g C-h. Finally, Section 5.5 gives a summary of the conclusions reached.

5.2 Sensitivity Decrease and Upward Zero-Drift as Functions of Dose Rate

5.2.1 Proposed Quantitative Theory of Sensor Response

Figure 4-4 shows that in the absence of a hydrogen-gas specimen, the indicated hydrogen concentration increases rather smoothly as a function of radiation level for dose-rate levels in excess of 2×10^7 erg/g C-h. The curves shown in Figure 4-1, which essentially represent the response to different samples

less the "zero response" given in Figure 4-4, fall off monotonically in the same range. The proposed explanation for such behavior is based on two factors which work in opposition to each other, viz., (1) a radiation-induced steady-state change in the effective pH of the electrolyte, and (2) the evolution of H_2 gas due to energy deposition in the electrolyte itself.

The evaluation of the effect of a given change in pH must start from the principle of operation of the electrolytic system. It is inferred from the discussion given in Reference 1 that the role of the anode is the same as that in a standard hydrogen half-cell. Molecules of H_2 are adsorbed on the platinum surface via the production of H-atom pairs. Before recombination and ejection can occur, H^+ ions, which are present in the electrolyte in the form of H_3O^+ (hydronium), attach themselves to the adsorbed H-atoms by virtue of exchange bonds in a process which is equivalent to the electroplating of metallic ions on a metal electrode of the same type. In the absence of another electrode, an effective current of H atoms into the anode, i_H, would therefore eventually lead to an anode potential ψ_o relative to the interior of the electrolyte. It is assumed that when the auxiliary electrode is in place, a current of negative ions results which sets up an electromotive field capable

of producing an ohmic drop in the external circuit (i.e., the input to the current amplifier) proportional to ψ_o.

Let ψ_o be the voltage between the anode and the interior of the electrolyte due to a net positive surface charge σ resulting from H^+ ions on the anode. Let i_H be the current density of H-atoms into the anode (which is just twice the current density of H_2 molecules into the anode). Let i_+ and i_- be the current densities of positive (H_3O^+) and negative ($SO_4^=$) ions to the anode respectively. Then for a steady state condition at the anode,

$$-i_H = i_+ = i_- \qquad (1)$$

where the negative coefficient of i_H signifies that the anode is taken to be at x = 0 so that the flow of both H_3O^+ and $SO_4^=$ ions is in the negative direction. (It is to be noted that i_H, i_+, and i_- are all <u>particle</u> currents.)

The net surface charge density on the anode in the steady state condition depends on the concentration of H_3O^+ ions in the electrolyte and on the relative velocities of the positive and negative ions in the field of the anode. Since Compton scatter electrons due to gamma rays and recoil protons due to neutrons are sure to destroy many H_2O molecules, thereby producing

H^+ and OH^- ions, it is reasonable to suppose that at high radiation levels the steady-state concentration of negative ions will exceed that in the unirradiated solution. The question, then, is what effect does this have on the anodic surface charge density σ and hence the external-current-inducing voltage ψ_o. The answer can be formulated by assuming the electrolyte to be electrically neutral and by relating the concentration of H_3O^+ at a given point in the electrolyte to the hydrogen current through Equation 1.

Let the H_3O^+ concentration at a radial distance x from the anode be c(x) and let the corresponding potential due to the anode be $\psi(x)$, where $\psi(x)$ goes to zero as x becomes large. If U is the velocity of the positive ions in a unit electric field, e is the electronic charge, k is Boltzman's constant, and T is the absolute temperature, the current density of H_3O^+ ions is

$$i_+ = -U \left(\frac{kT}{e} \frac{dc}{dx} + c \frac{d\psi}{dx}\right) \qquad (2)$$

Equation 2 expresses the fact that the ion current depends on both the electric field due to the anode and (because of diffusion) on the gradient of a non-uniform ion distribution c(x) (see, for example, Ref. 2, from which the above symbols were taken). Equation 2 together with the first part of Equation 1 gives

$$-U\left(\frac{kT}{e}\frac{dc}{dx} + c\frac{d\psi}{dx}\right) = -i_H \qquad (3)$$

where in a diffusion-limited condition $-i_H$ is independent of c(x) and depends only on the properties of the membrane and on the external hydrogen concentration.

In order to calculate σ in terms of c(x), one needs a solution of Equation 3 that holds near x = 0. It is seen by inspection that if $c_o = c(0)$ is the concentration at the anode and $c_1 = c(\infty)$ is the concentration far from the anode, one such solution has the form

$$c(x) = ax + c_o, \quad \psi(x) = K \ln\left(\frac{ax + c_o}{c_1}\right) \qquad (4)$$

provided that

$$-U\left(\frac{kT}{e} + K\right) a = -i_H \qquad (5)$$

The parameters K and a can be determined simultaneously by making use of the equation corresponding to Equation 2 for the negative ions. If the velocity of the negative ions is V, then the current density of negative ions of average valance number n is

$$i_- = -\frac{1}{n} V\left(\frac{kT}{ne}\frac{dc}{dx} - c\frac{d\psi}{dx}\right) \qquad (6)$$

where use has been made of the assumption that at each point the positive and negative ion concentration have the same value c(x). Thus, when Equation 4 is valid,

$$i_- = -\frac{1}{n} V\left(\frac{kT}{ne} - K\right) a \qquad (7)$$

Also,

$$i_+ = -U \left(\frac{kT}{e} + K\right) a \tag{8}$$

Use of Equations 7, 8, and the second part of Equation 1 yields

$$K = -\left(\frac{n^2U - V}{V + nU}\right) \frac{kT}{ne} \tag{9}$$

and from Equations 9 and 5,

$$a = \left[\frac{V + nU}{(n + 1)\ UV}\right] \frac{ne}{kT}\ i_H \tag{10}$$

It is seen that the behavior of both the H_3O^+ concentration $c(x)$ and the potential $\psi(x)$ are given at points near the anode by Equation 4 together with Equations 9 and 10; then the surface charge density on the anode can be expressed in terms of the as yet undetermined boundary concentration c_o by means of the relation

$$\sigma = - E_o \left(\frac{\partial \psi}{\partial x}\right)_o \tag{11}$$

where E_o is the electrical permitivity of the electrolyte and where use has been made of the fact that the field within the anode is zero. From Equations 4, 9, 10, and 11,

$$\sigma = E_o \frac{n^2U - V}{(n + 1)\ UV} \frac{i_H}{c_o} \tag{12}$$

where the temperature dependence has cancelled out.

Given the surface charge density of the anode, it should be possible to calculate the potential of the anode with respect to infinity by evaluation the field at each point and integrating the work elements from infinity. Although, inasmuch as the anode

is not a point, this would be a difficult process, one can merely observe that the result will be proportional to σ and express the potential at a point x as

$$\psi(x) = \sigma G(x) \tag{13}$$

where G(x) depends only on the geometry of the electrode system. In particular at the anode surface, one can define $G_o = G(0)$ and obtain for the potential of the anode surface with respect to infinity

$$\psi_o = \sigma G_o \tag{14}$$

or, from Equation 12,

$$\psi_o = E_o G_o \left[\frac{n^2 U - V}{(n + 1)\ UV}\right] \frac{i_H}{c_o} \tag{15}$$

It is now desirable to express c_o in Equation 15 in terms of a more readily observable concentration, namely that which exists far from the perturbing influence of the anode. In the development given thus far it has been assumed that c(x) varies linearly from c_o near the anode. The reason for its varying at all is, of course, that the more rapidly moving positive ions tend to be repelled from the anode. In order to describe the variation of ion density as a function of distance from the anode, use will be made of the familiar result from statistical mechanics that the distribution n(x,y,z) of a system of ions in a conservative field defined by a potential $\phi(x,y,z)$ is given by

$$n(x,y,z) = n(\infty) \exp - e\phi(x,y,z)/kT) \tag{16}$$

Although this result is derived from the assumption that the system is in equilibrium, it is assumed here that it also applies to the steady-state situation of interest (this is equivalent to assuming that the current i_+ is small compared to the total ion flux in the electrolyte). Hence, if c_1 is the concentration far from the anode,

$$c(x) = c_1 \exp(-e\psi(x)/kT) \tag{17}$$

and in particular

$$c_o = c_1 \exp(-e\psi_o/kT) \tag{18}$$

Combination of Equations 15 and 18 gives the transcendental relation

$$\psi_o = E_o G_o \frac{n^2U - V}{(n+1)UV} \frac{i_H}{c_1} \exp(e\psi_o/kT) \tag{19}$$

which in principle can be solved to yield the desired connection between ψ_o and c_1. In order to obtain a facile solution of Equation 19, it can be observed that if the hydrogen-atom current density to the anode, i_H, is sufficiently small, then the ratio $(c_1 - c_o)/c_1$ must be small. Then Equation 18 implies that if i_H is sufficiently small, the ratio $e\psi_o/kT$ must be much less than unity. For this condition, Equation 19 becomes

$$\psi_o = E_o G_o \frac{n^2U - V}{(n+1)UV} \frac{i_H}{c_1} \left(1 + \frac{e\psi_o}{kT}\right) \tag{20}$$

which gives

$$\psi_o = \frac{E_o G_o \frac{n^2U - V}{(n+1)UV} \frac{i_H}{c_1}}{1 - E_o G_o \frac{n^2U - V}{(n+1)UV} \frac{e}{kT} \frac{i_H}{c_1}} \tag{21}$$

The second term in the denominator of Equation 21 is always positive. It is therefore clear that ψ_o is small when i_H is small, as expected. If it is also assumed that the detector operates in its linear range, then Equation 21 reduces to

$$\psi_o = \alpha \frac{i_H}{c_1} \tag{22}$$

where

$$\alpha = E_o G_o \frac{n^2U - V}{(n+1)UV} \tag{23}$$

Equation 22 is the desired approximate expression for ψ_o, the voltage induced by hydrogen adsorption on the anode when the device functions within its normal range of operation. The physical significance of the dependence of ψ_o on i_H, the hydrogen current to the anode, and c_1, the ion concentration in the electrolyte, is discussed below.

5.2.2 Effect of Radiation on the Overall Response

The analysis of the response of the hydrogen detector to radiation will be based on Equation 22. The validity of this equation depends on the assumption that i_H is small, both through Equations 17 and 20. Also inherent in the whole derivation is

the assumption that both i_H and c_1 are in the range where the operation is diffusion limited. For example, it could not be inferred from Equation 22 that making c_1 arbitrarily small would lead to a substantially higher ψ_o, since eventually i_H in Equation 3 would become a function of c_1 and ψ_o would fall off due to the reduction of hydrogen ion current to the anode. On the other hand, if the effect of radiation is to <u>increase</u> c_1, the diffusion limited condition will be abetted and Equation 22 will still apply. In this situation, an increase in c_1 causes a corresponding increase in negative-ion concentration and a given positive ion on the anode will be neutralized more rapidly so that the steady state ψ_o will decrease, as indicated by Equation 22.

Two possible effects of radiation are (1) an increase in c_1 due to the production of hydrogen ions in the electrolyte, and (2) an increase in i_H due to radiation-induced H_2. The latter is expected to mainly result from energy deposition in the electrolyte itself since the rate of diffusion of H_2 produced in the organic housing is expected to be slow. Another possible effect of radiation is the variation of n, the average valence number of the negative ions, and V, the velocity of the negative ions in a unit electric field. Changes in these numbers, and hence in α, could result if the steady state concentration of OH^- ions approached that of the $SO_4^=$ ions. However, such changes are

expected to be minor for the following reasons. Since the positive-ion velocity, U, is expected to be substantially larger than V, one can write approximately

$$\alpha = E_o G_o \frac{n^2}{n+1} \frac{1}{V} \tag{24}$$

with n between 1 and 2. Now V itself is proportional to n so that other things being equal, the α for equal concentrations of OH^- and $SO_4^=$ is less than that for pure $SO_4^=$ by only 10%. Although V is also inversely proportional to the ionic radius, such radii do not usually differ greatly from one another. For example, the radius of $S^=$ is given as 1.84 $\mathring{A}$, whereas that of H^- is 2.08 $\mathring{A}$. It is concluded that α is approximately independent of the ion concentration.

Similar considerations show that the effect of radiation on the resistivity of the electrolyte is not great enough to warrant detailed investigation. Since the conductivity is limited by the flow of Cu^{++} ions and since V is proportional to n, it follows that the contribution of an $SO_4^=$ ion to the current is four times that due to an OH^- ion so that even for equal concentrations the effect of OH^- is to decrease the resistivity by only about 25%. It is therefore assumed that the effect of radiation on r, the total impedance (internal + external) of the input to the current amplifier, can be ignored.

The ultimate effect of ψ_o is to create an electromotive field which in turn produces a current density to the current amplifier which is proportional to ψ_o and inversely proportional to r. Then if the amplification factor (meter reading per unit induced voltage per unit anode surface area) is defined as A/r and if a_H is the area of the anode, the response indicated by the meter is

$$I = \frac{A}{r} \; a_H \; \psi_o = (\frac{A}{r} \alpha) \; a_H \; \frac{i_H}{c_1} \qquad (25)$$

where use has been made of Equation 22. In the preceding treatment no allowance has been made for the effect of the radiation on H_3O^+ and $SO_4^=$ already in the electrolyte. This omission is reasonable since, for the radiation fields envisaged, only a small fraction of such ions will be effected. The H^+ and OH^- ions produced from the water are only significant because the number of water molecules present greatly exceed (by a factor of about 10^3) the number of ions.

Equation 25 says that the response is proportional to $a_H i_H$, the total hydrogen atom current to the anode, and inversely proportional to c_1, the hydrogen ion concentration. In order to predict the effect of a radiation field, one must take some model for the change of i_H and c_1 as a function of radiation level. Experience with the irradiation of all sorts of hydrogenous materials indicates that the rate of H_2 evolution due to

radiation is simply proportional to $\dot{E}$, the rate of energy deposition. It will be shown that this implies a linear variation of i_H with $\dot{E}$. On the other hand, the effect of radiation on c_1 depends on factors such as recombination rates which may themselves depend on c_1.

The most probable first step in the deposition of energy by radiation in aqueous solutions is the direct or indirect production of water molecules in highly excited states designated by H_2O^*. Such molecules may react with stable molecules either by de-exciting or by yielding protons to form OH^- and H_3O^+. It is to be expected that the latter process will be greatly catalyzed by the presence of any ions already in the solution (see, for example, Ref. 3). A reasonable description of the secondary step in radiation-induced ionization is therefore

$$H_2O^* + H_2O + H_3O^+ \rightarrow OH^- + H_3O^+ + H_3O^+ \qquad (26)$$

The rate of removal is presumably controlled by the number of ions with which recombination can occur. Then if c_1' designates the excess hydrogen-ion concentration due to radiation, the steady-state condition takes the form

$$\frac{dc_1'}{dt} = P\dot{E}\, c_1 - Rc_1'\, c_1 = 0 \qquad (27)$$

where P is the production coefficient for H_2O^* molecules and R is the removal coefficient for H_3O^+ ions. Equation 27 implies that the concentration c_1 as a function of radiation level is given by

$$c_1(\dot{E}) = c_1(0)\ (1 + \mu\dot{E}) \tag{28}$$

where

$$\mu = \frac{P}{Rc_1(0)} \tag{29}$$

The validity of Equation 28 can, of course, only be justified in terms of comparisons with experimental data. That is, the proposed reaction mechanisms can only be regarded as realistic if a value of μ can be found such that Equation 28 and 22 predict the observed decrease in sensitivity of the sensor as a function of radiation level.

5.2.3 Effect of Radiation on the Zero-Corrected Response

In order to determine whether Equation 28 is in accord with the data, Equation 25 will be used to calculate the "zero-corrected" response, i.e., the difference between I', the response in the presence of a given hydrogen sample, and I'', the response in the absence of a hydrogen sample. This comparison eliminates the effect of radiation-induced H_2 molecules. From Equations 25 and 28 it is seen that the zero-corrected response should be

$$I'(\dot{E}) - I''(\dot{E}) = \frac{I}{(1 + \mu\dot{E})} \tag{30}$$

where I is the response to the given sample in the absence of radiation. In the absence of any information on P/R, one can only hope to justify Equation 28 by finding a μ such that Equation 30 gives a reasonable fit to the measured data.

The zero-corrected experimental data as a function of dose rate shown in Figure 4-1 are replotted in Figure 5-1; also shown are fits corresponding to Equation 30 with $\mu = 1.14 \times 10^{-9}$ $(\text{erg/g C-h})^{-1}$. Although the experimental points are badly scattered, it appears that Equation 30 can give about as good a fit to the data as can be made. It is therefore tentatively concluded that the considerations leading to Equation 30 explain the loss of sensitivity in zero-corrected response with increasing levels of radiation.

5.2.4 Analytical Interpretation of Zero Drift

The upward drift of the indicated response $I''(\dot{E})$ with no sample gas as a function of $\dot{E}$, shown in Figure 4-4, cannot be explained in terms of changes in ion concentration. Indeed, Equation 25 shows that if no H_2 were evolved in the electrolyte, $I''(\dot{E})$, the response in the absence of sample H_2, would be zero for all radiation levels. However, it is known that radiation produces H_2 molecules in all hydrogenous materials. If it is assumed that H_2 diffusion out of the organic housing is too slow to be of importance, then $I''(\dot{E})$ is determined by the H_2 evolution

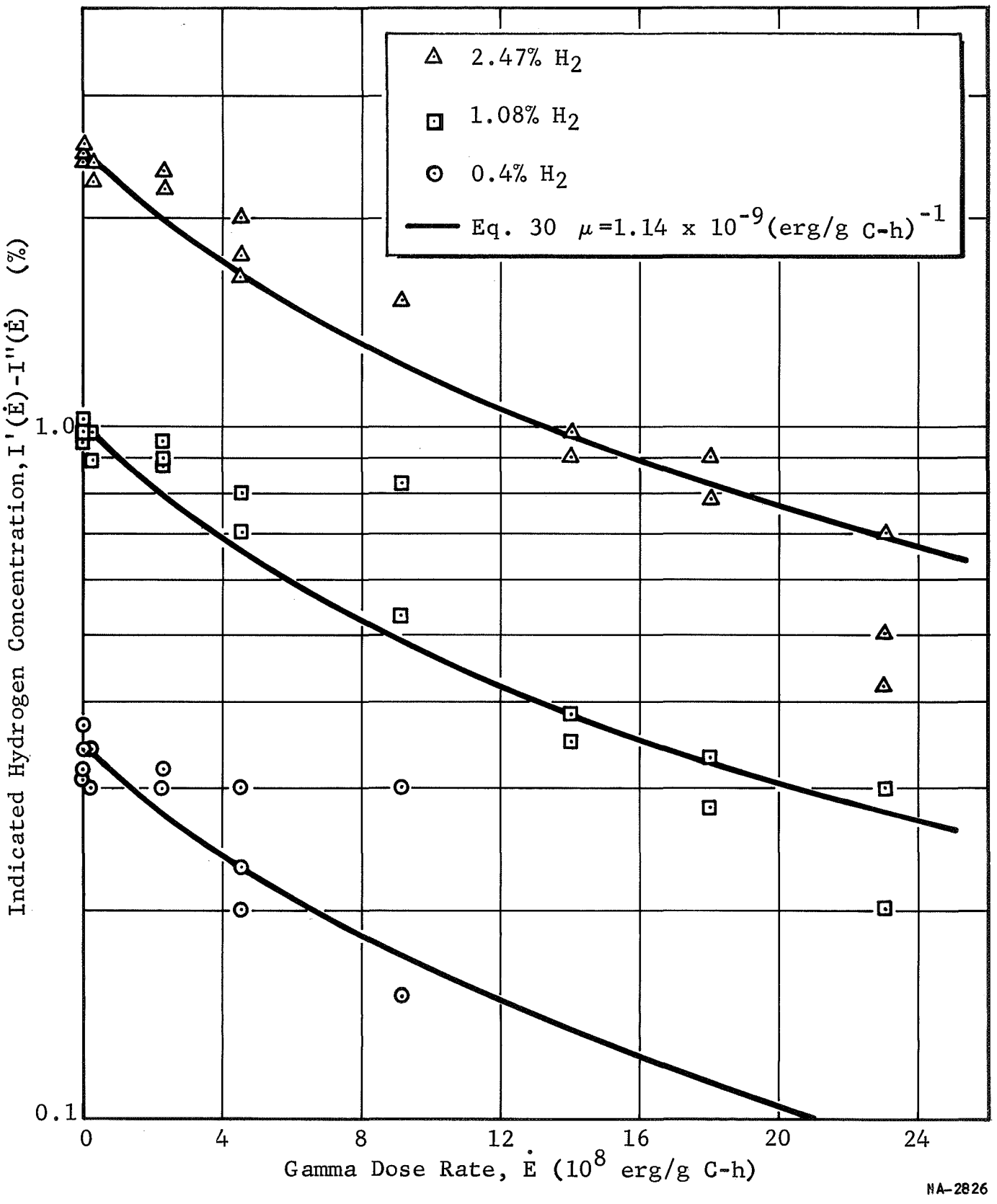

Figure 5-1 Zero-Corrected Response as a Function of Gamma Dose Rate

in the 0.25-cm^3 electrolytic reservoir together with the change in c_1. It will be clear from the discussion below that once an H_2 molecule finds itself inside the electrolyte the chance of its diffusing back through the membrane before being adsorbed on the anode is negligible. Therefore, if one knew the g-value (number of H_2 molecules evolved per unit mass per 100 eV) for water, the main constituent of the cell, the hydrogen atom current to the anode would be

$$a_H i_H = g \dot{E} M \tag{31}$$

where M is the mass of the electrolyte. The other parameters in Equation 25 can also be calculated: $(A\alpha/r)$ from the response in the absence of radiation, and $c_1(\dot{E})$ from the μ value obtained above. It should therefore be possible to make an ab initio calculation of $I''(\dot{E})$ if g is given. However, since the experimental data on g for water are in some doubt, the procedure here will be to calculate $(A\alpha/r)$ and $c_1(\dot{E})$ and then try to find a g that will conform to the experimental data on $I''(\dot{E})$ shown in Figure 5-2. The extent to which the g agrees with those in the literature can then be taken as an indication of the validity of the overall theory.

In the absence of radiation, the hydrogen-ion concentration $c_1(0)$ can be estimated from the assumption of total dissociation. Although 0.1 N H_2SO_4 in pure water would imply a dissociation

constant of only 0.63, the presence of $CuSO_4$ ions should cause the dissociation constant to be closer to unity. It is therefore assumed that

$$c_1(0) = 0.10 \text{ moles/liter} = 1.0 \times 10^{-4} \text{ moles } H^+/cm^3 \qquad (32)$$

The current $a_H i_H$, corresponding to a given meter response I, can be calculated by estimating the actual rate of diffusion of H_2 molecules through the membrane for a given sample concentration. To this end the diffusion coefficient D for H_2 molecules in the membrane is calculated using the equation for the time constant t_c given in Reference 1:

$$t_c = \frac{(\Delta x)^2}{D} \qquad (33)$$

Taking the membrane thickness as $\Delta x = 1$ mil $= 0.0025$ cm and $t_c = 1.3$ sec (the exponential time constant inferred from the data) gives

$$D = 7 \times 10^{-6} \text{ cm}^2/\text{sec} \qquad (34)$$

which for any reasonable velocity of H_2 inside the membrane implies a very low transmission probability T for a membrane 0.0025 cm thick. In this case ($T \ll 1$), it can be shown that

$$T = 4(D/v)/\Delta x \qquad (35)$$

where v is the average velocity of H_2 molecules in the membrane. If v is taken to be the velocity of H_2 molecules in a dilute

gas at ordinary temperature, then Equation 35 gives

$$T = 0.8 \times 10^{-7} \tag{36}$$

which proves the assertion that once H_2 molecules are in the electrolyte they are adsorbed on the anode. If the membrane is exposed to an H_2 concentration N_{H_2} (molecules/cm^3) and if the area of the membrane exposed is taken as a_H, the area of the anode (which is approximately the case), then

$$a_H i_H = (1/4)v\ (2N_{H_2})a_H\ T \tag{37}$$

Evaluation of Equation 37 for the N_{H_2} corresponding to 1 atmosphere of hydrogen at 300°K (so that I" (0) = 1) gives

$$a_H i_H = 2.6 \times 10^{15}\ \text{H atoms/sec} = 4.0 \times 10^{-4}\ \text{amp} \tag{38}$$

where for convenience of comparison the H-atom current has been translated into the number of ampere-equivalents of current flowing to the anode in the form of hydrogen ions. Substitution of I"(0) = 1 along with the values given in Equation 32 and Equation 38 into Equation 25 gives

$$(A\alpha/r) = 0.25\ \text{amp}^{-1}\ \text{moles/cm}^3 \tag{39}$$

It was shown above that $\mu = 1.14 \times 10^{-9}$ (erg/g C-h)$^{-1}$ gives a reasonable explanation of the zero-corrected data. If one takes this value together with $c_1(0) = 1.0 \times 10^{-4}$ moles/cm^3 from Equation 32, then Equation 28 gives

$$c_1(\dot{E}) = 1.0 \times 10^{-4} + 1.14 \times 10^{-13}\ \dot{E} \tag{40}$$

where $c_1(\dot{E})$ is in moles/cm^3 and $\dot{E}$ in erg/g C-h. Then from Equations 25, 39, and 40,

$$I(\dot{E}) = 0.25 \frac{a_H i_H}{1.0 \times 10^{-4} + 1.14 \times 10^{-13} \dot{E}} \quad (41)$$

where the total hydrogen-atom current to the anode, $a_H i_H$, is expressed in ampere-equivalents. Equation 41 should hold in the general case where part of the hydrogen current to the anode is due to diffusion through the membrane and part due to radiation-induced evolution in the electrolyte. In the case where the sample concentration is 0%, $a_H i_H$ is given by Equation 31. If the mass of the 0.25 cm^3 of electrolyte is taken to be 0.25 grams, and if g is expressed in H_2 molecules/100 eV as is usual, then the hydrogen current (per second) to the anode is

$$a_H i_H = g(0.25\dot{E}/3600)/(1.60 \times 10^{-12})(100) \quad (42)$$

or, in terms of ampere-equivalents,

$$a_H i_H = (1.4 \times 10^{-13})\dot{E}\, g \quad (43)$$

Therefore, the response for the case of a 0% sample should be

$$I''(\dot{E}) = (0.25) \frac{(1.4 \times 10^{-13}) g\, \dot{E}}{1.0 \times 10^{-4} + 1.14 \times 10^{-13} \dot{E}} \quad (44)$$

The meter response for 0% hydrogen shown in Figure 4-4 is replotted on a linear scale in Figure 5-2, along with the evaluation of Equation 44 for g = 0.09 H_2 molecules/100 eV (which

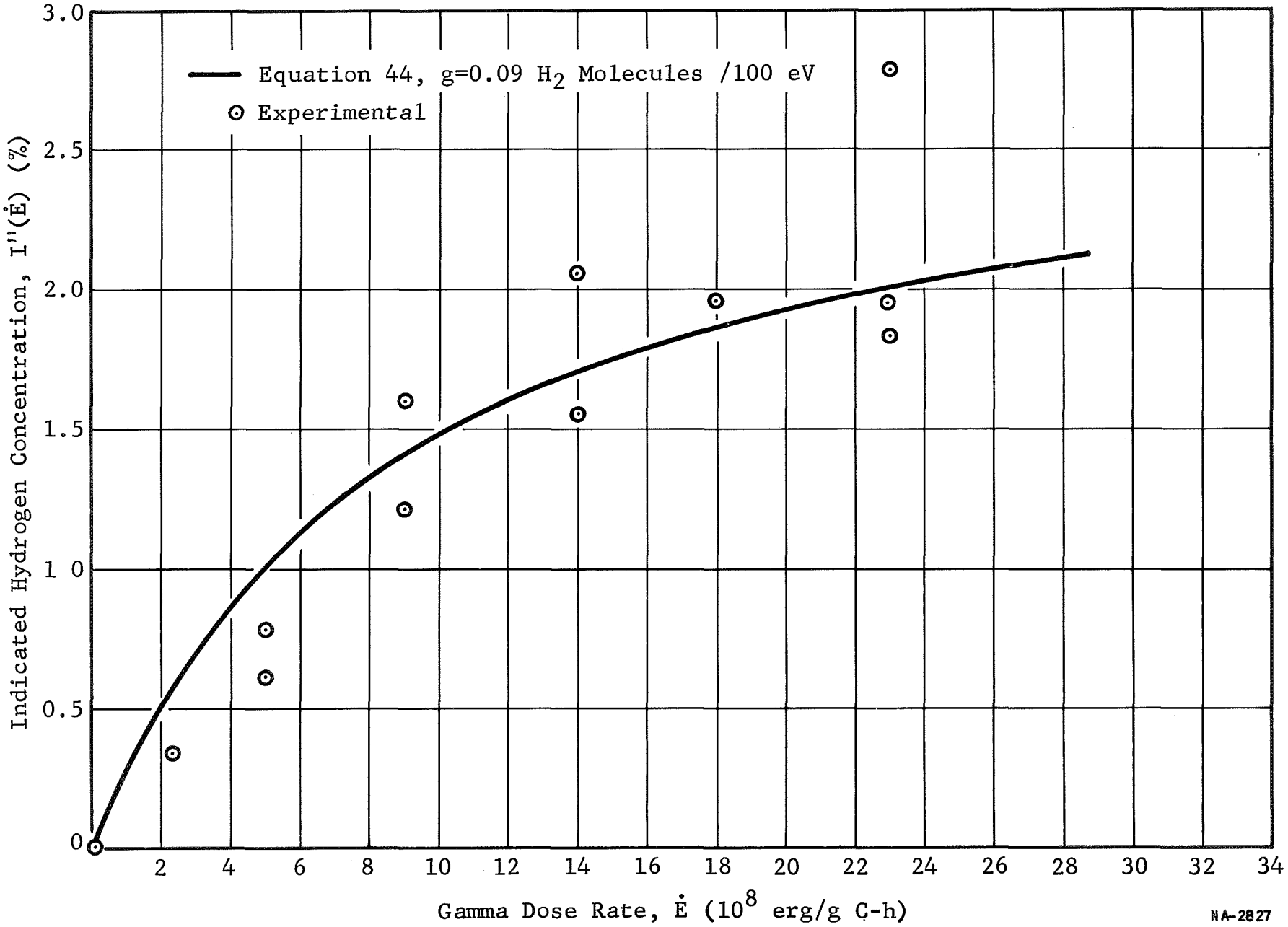

Figure 5-2 Calculated and Experimental Response Without Hydrogen Sample

value does not necessarily give the best fit). The agreement is as good as could be expected in view of the many approximations involved. Three features of the comparison are noteworthy. The first is that had the variation in c_1 not been taken into account, the calculated results would have been curves of constant slope, which would be hard to reconcile with the data. Second, if an attempt had been made to find a value of μ which would give the best overall agreement in Figures 5-1 and 5-2, a better prediction of the more numerous lower values in Figure 5-2 would have resulted. Third, the g value of ice warmed up after irradiation at 70°K is found to be g = 0.1 H_2 molecules/100 eV (Ref. 4) in good agreement with the inferred g = 0.09. The reason for attaching any significance to the latter results in this connection is that H-atoms are mobile at 70°K and should therefore form H_2 molecules at about the same rate as in water. Although no data on the g value of water in the liquid state have yet been located, it is tentatively concluded that the theory presented above is in reasonable quantitative agreement with all of the experimental results.

In closing the subject of sensitivity and zero drift as a function of radiation level, it is well to note that in comparing the response with gamma dose rate a certain fraction of energy deposited in the electrolyte has been neglected. On the basis

of measured neutron fluxes and assumed spectra, it is estimated that hydrogen recoils in the electrolyte constitute an energy deposition rate equal to about 25% of the gamma dose rate. Allowance for this effect in the above comparisons would only introduce a minor scaling factor and would have no effect on the apparent success of the analysis.

5.3 Other Effects Observed

The most probably explanation of the observed increase in zero-instability with increasing exposure rate appears to be the effect of temperature fluctuations on the steady-state hydrogen-ion concentration. The temperature of the copper plate over the membrane was observed to vary by as much as 15°F during the experiment and in a way which was not correlated with the temperature of the sensor housing. This implies that the electrolyte was subjected to considerable temperature variations which may well have been out of phase with those of the copper plate because of the relatively high specific heat of the electrolyte.

Although temperature variation in the electrolyte could have little effect on the rate of evolution of H_2 gas, it is to be expected that a 10°F change could cause the rate constant for hydrogen-ion production through the indirect process assumed in Equation 26 to vary by an order of magnitude. An increasing

zero-instability with increasing radiation rate is therefore a logical consequence of the theory proposed to explain the loss of zero-corrected sensitivity and zero drift. For a 0% hydrogen sample, the sensor responds to hydrogen gas which is evolved in the electrolyte at a rate independent of temperature. Once the meter has been adjusted to zero, it would remain there if the hydrogen-ion concentration were constant, since the current of internally produced H-atoms to the anode is independent of temperature. However, at high radiation levels (on the order of 10^9 ergs/g C-h), the excess hydrogen-ion concentration due to radiation becomes comparable to that of the unirradiated electrolyte. Under this condition, it is estimated from Figure 5-2 that a factor of two decrease in excess concentration caused by a temperature change of several degrees would result in an apparent indication of more than 1% hydrogen. Unfortunately, since the temperature of the electrolyte could not be monitored, it is not possible to make even a qualitative check on this supposition.

A rapid recovery of performance after irradiation would be expected in terms of the above theory, since in the absence of radiation, both evolved hydrogen and excess hydrogen ions should vanish almost immediately. Such a rapid recovery was observed after the last shutdown but not after the first one.

The reason for the difficulty with response times was, of course, that due to the zero-instability it was impossible to assign a final asymptotic response for a given reading. It is likely that the gas bubble observed several days after the irradiation evolved as a result of evaporation and does not relate to any other effects observed except for the high impedance which is attributed to loss of electrolyte.

It should be noted that none of the effects cited above constitutes a problem which is beyond remedy. Comparison of the theoretical and experimental results shows that, in a sense, the device worked properly at all radiation levels. There is no indication that the response was nonlinear; the drifts and fluctuations that occurred resulted from radiation effects and temperature variations which changed the properties of the electrolyte, but such changes were apparently confined to a range corresponding to a stable response to external hydrogen gas.

5.4 Use of Sensor in High-Level Radiation Fields

The experimental data indicate that some problems will be encountered in the operation of the sensor for dose-rate levels in excess of 2×10^7 erg/g C-h. In light of the foregoing analysis, the following suggestions might be considered as a means of improving its performance at higher dose rates:

a. A pair of sensors might be used in opposition, with one exposed to the hydrogen sample and one sealed against external hydrogen. In this way the current to the current amplifier resulting from radiation effects in the electrolyte would be annuled.

b. A more uniform method of temperature control should be utilized.

c. The sensor can, of course, be shielded.

d. The sensor, except for the membrane, could be fabricated of ceramic.

5.5 Summary of Analytical Conclusions

a. The observed decrease in zero-corrected sensitivity is due to a radiation-induced steady-state increase in the negative-ion concentration of the electrolyte.

b. The observed upward drift of response with increasing radiation levels in the absence of hydrogen sample is due to the radiation-induced evolution of H_2 gas in the electrolyte.

c. Instability of response at high dose rates resulted from temperature fluctuations which affected the rate constant for radiation-induced ion production in the electrolyte.

d. In spite of the drifts and fluctuations, the sensor continued to perform within its linear range of operation at high dose rates.

e. For use in radiation fields in excess of 2×10^7 erg/g C-h, consideration should be given to (1) using a pair of analyzers in opposition and, (2) providing a more uniform temperature control by means of a coolant bath; it is recommended that another experiment be run implementing these suggestions.

REFERENCES

1. Harman, J. N., Design, Development and Fabrication of a Prototype Eight Channel Hydrogen Gas Concentration Monitoring System, Beckman Instruments, Inc. Report FR-2378-101, 30 June 1966.

2. Rutgers, A. J., Physical Chemistry (Interscience Publishers, Inc., New York, 1954), p. 249.

3. Schwab, G., et al, Catalysis (D. Van Nostrand Company, Inc., New York, 1937), p. 20, et seq.

4. Siegel, S., et al., "Irradiation Yields of Radicals in Gamma-Irradiated Ice at 4.2° and 77°K", J. Chem. Phys. 34, 1961, pp. 1782-1788.

DISTRIBUTION

ADDRESSEE	NO. OF COPIES
AFWL, Research and Technical Division Air Force Systems Command Kirtland AFB, New Mexico Attn: Maj. C. L. Schra (WLDA-2)	5
Headquarters, USAF The Pentagon Washington, D. C. Attn: Mr. W. D. Downs (AFRNE-B)	1
SNPO-Cleveland Lewis Research Center 21000 Brookpark Road Cleveland 35, Ohio Attn: Mr. L. R. Nichols	5
SNPO-Washington Division of Reactor Development U. S. A. E. C. Germantown, Maryland Attn: Mr. J. Morrissey	1
Aerojet-General Corporation P. O. Box 15847 Sacramento, California Attn: Mr. D. E. Deutsch	5
Aerojet-General Corporation P. O. Box 15847 Technical Library Bldg. 2015, Dept. 2410 Sacramento, California	1
Westinghouse Astronuclear Laboratory P. O. Box 10864 Pittsburgh, Pennsylvania Attn: Mr. H. P. Perkins	3

DISTRIBUTION

ADDRESSEE	NO. OF COPIES
SNPO-C Resident Office Aerojet-General Corporation Sacramento, California Attn: Mr. J. J. Fitts	1
Radiation Effects Information Center Battelle Memorial Institute 505 King Avenue Columbus, Ohio	1

GENERAL DYNAMICS

Fort Worth Division